https://doi.org/10.5194/egusphere-2025-3167
Preprint. Discussion started: 25 July 2025

Eight years of continuous Rockall Trough transport observations using moorings and gliders

Kristin Burmeister[1], Neil J. Fraser[1], Sam C. Jones[1], Stuart A. Cunningham[1,2], Lewis A. Drysdale[1], Mark E. Inall[1], Tiago S. Dotto[3], and N. Penny Holliday[3]

[1]SAMS Scottish Association for Marine Science, Oban, United Kingdom
[2]University of the Highlands and Islands, United Kingdom
[3]NOC National Oceanography Centre, European Way, Southampton, SO14 3ZH, UK

Correspondence: Neil J. Fraser (neil.fraser@sams.ac.uk)

Abstract. The Rockall Trough (RT) channels an important branch of the North Atlantic Current (NAC), transporting heat from the Gulf Stream toward the Nordic Seas, and the European Slope Current (ESC) which flows northward along its eastern boundary. Variability in the NAC influences poleward heat transport and the strength of the Atlantic Meridional Overturning Circulation, while the ESC plays a key role for the oceanic conditions on the European shelf and the North Sea. Here we present observed volume, heat, and freshwater transports through the Rockall Trough from 2014 to 2022, using data from Ellett Array moorings (operational since 2014) and gliders (deployed from 2020 onward). Although gliders provide high-resolution spatial data in the ESC, their inconsistent temporal coverage complicates their integration into RT transport estimates. We develop a methodology to merge mooring and glider observations into a unified, high-resolution time series, producing—for the first time—a continuous ESC transport dataset spanning nearly a decade. This demonstrates the effectiveness of heterogeneous observing arrays and provides a transferable framework for sustained ocean transport monitoring.

https://doi.org/10.5194/egusphere-2025-3167
Preprint. Discussion started: 25 July 2025

1 Introduction

The poleward transport of oceanic heat and salt in the North Atlantic is a critical component of the global climate system and plays a major role in regulating the European temperature. The Rockall Trough (RT), a 200 km wide channel in the eastern subpolar North Atlantic, serves as a key pathway for both the North Atlantic Current (NAC) and the European Slope Current (ESC). These currents have an order-one downstream impact on physical and biogeochemical conditions in the Arctic, Nordic Seas, North Sea and Northwest European Shelf (Berx et al., 2013; Marsh et al., 2017; Porter et al., 2018). Recent results indicate that the circulation in the RT plays a primary role in the variability of the subpolar overturning circulation (Fu et al., in review), while NAC buoyancy loss to the atmosphere is the biggest water mass transformation signal in the subpolar gyre (Jones et al., 2023).

There is a longstanding effort to monitor the circulation and hydrography in the RT, exploiting this natural bottleneck in North Atlantic circulation (e.g. Ellett et al., 1986; Holliday and Cunningham, 2013). Regular hydrographic surveys on the Ellett Line, a section across the northern RT, commenced in 1975, while a southern RT section has been running since 2006 (Daly et al., 2024). Since 2014, RT transports on the Ellett Line have been continuously monitored using a dynamic height mooring array (Figure 1) deployed as part of the larger OSNAP (Overturning in the Subpolar North Atlantic) programme (Houpert et al., 2020; Lozier et al., 2019). While the mooring array accurately constrains the volume transport in the RT mid-basin, difficulties have arisen at the RT boundaries where narrow jets over steep topography exhibit high spatiotemporal variability and are less suited to moored observations. In particular, the ESC is situated at the eastern boundary and hence not fully captured by the Ellett Array (Figure 1). Continuous records of transport in these boundary "wedges" have relied upon the spatial and temporal extrapolation of velocity observations together will numerical model output (Houpert et al., 2020). A bottom-mounted acoustic Doppler current profiler (RTADCP) was deployed in the ESC core when the RT mooring array was launched in 2014 but the instrument was lost through trawling activity after around 8 months, highlighting the difficulties conducting long-term monitoring of the ESC using moored platforms.

Although the ESC volume transport is small compared to the NAC, it carries warm and salty Eastern North Atlantic Water directly adjacent to the Northwest European Shelf break and therefore has a disproportionate impact on conditions on the shelf (Porter et al., 2018; Jones et al., 2020) and in the North Sea (Marsh et al., 2017). In the last few decades several studies have made moored observations of the ESC velocity (summarised in Diabaté et al., 2025), however these are generally short-term process studies rather than long-term climate monitoring efforts. It is essential that the RT observing system can accurately capture the evolving ESC velocity and transports.

Since 2020, underwater gliders have been deployed to take repeat sections of the RT eastern wedge. Between April 2020 and February 2023, the gliders amassed 166 transects across 7 glider missions, with a nominal temporal resolution of 3 days between transects and some longer gaps between glider missions. Fraser et al. (2022) developed an along-isobath transformation to map these spatially scattered data onto the Ellett Array section grid, allowing for the hydrography and velocity fields from each glider transect to be analysed on a consistent gridded section while preserving volume transport and property transports. This analysis has given an unprecedented insight into the strength, structure, and seasonality of the ESC, and gives a directly

https://doi.org/10.5194/egusphere-2025-3167
Preprint. Discussion started: 25 July 2025

observed eastern wedge transport estimate which complements the mid-basin transports observed by the moorings of the Ellett Array (Figure 1). However, while Fraser et al. (2022) address the spatial scatter of glider data, the gridded transects remain scattered and often sparse over time. To become truly integrated into the climate monitoring effort, glider observations must provide a continuous transport time series.

In this study we present an 8-year record of observed volume, heat and freshwater transports in the RT. We construct a continuous RT eastern wedge velocity product combining the high temporal resolution of the moored observations and the high spatial resolution of the glider sections. We demonstrate that this improves the spatial and temporal representation of the ESC in the RT transport time series. The methods we develop in this study are directly applicable to the more general problem of ocean transport monitoring using a heterogeneous array of mooring and glider platforms.

2 Data and methods

2.1 Glider observations

Seven consecutive Seaglider missions occupied the eastern RT boundary region during the periods April–August 2020, October 2020–January 2021, April–May 2021, October 2021–February 2022, April 2022, July 2022-September 2022, November 2022-February 2023. The instruments completed a total of 166 repeat transects between the approximate EB1 mooring location and the 200 m isobath to the east (cross-hatched region in Figure 1). The glider observes temperature, salinity and pressure between the surface and the seabed up to a maximum depth of 1000 m (Fraser et al., 2022).

The seagliders are equipped with a SBE41 CTD, which has an accuracy of 0.0035 PSU, 2dbar and 0.002°C and a typical stability of 0.0011 PSU per year, 0.8 dbar per year and 0.0002°C per year for salinity, pressure and temperature, respectively. The glider navigates with a magnetic compass under water and obtains a GPS position fix each time it surfaces. Depth-Avaraged Current (DAC) can be derived based on any deflection off course between two consecutive GPS fixes (Fraser et al., 2022). Coefficients of the gliders hydrodynamic flight model (Eriksen et al., 2001) were re-calculated after each mission by selecting a subset of dives and iteratively comparing the vertical velocity predicted by the flight model against the vertical velocity implied by the pressure sensor. The corrected flight model was then used to remove thermal inertia effects on the CTD sensor. Temperature and salinity data were post-processed using GliderTools (Gregor et al., 2019).

Fraser et al. (2022) introduced a methodology to calculate volume transports for the upper 1000m of the eastern wedge based only on glider observations. Glider transects are invariably affected by the ocean velocity field and hence follow irregular and inconsistent trajectories. The different transects do not correspond spatially and do not in general have the same cross-sectional area. To overcome this issue, all transects are projected onto a common section approximately perpendicular to isobaths using an along-isobath transformation. The underlying assumption is that ESC streamlines follow isobaths and tracers are conserved along isobaths within the area of the glider observations. We outline this methodology only briefly here; a detailed desription can be found in Fraser et al. (2022):

For temperature and salinity, this transformation takes in situ observations on the glider path and assigns them to the corresponding isobath on the common section. DAC observations require a more subtle treatment. First, the component of the DAC

https://doi.org/10.5194/egusphere-2025-3167
Preprint. Discussion started: 25 July 2025

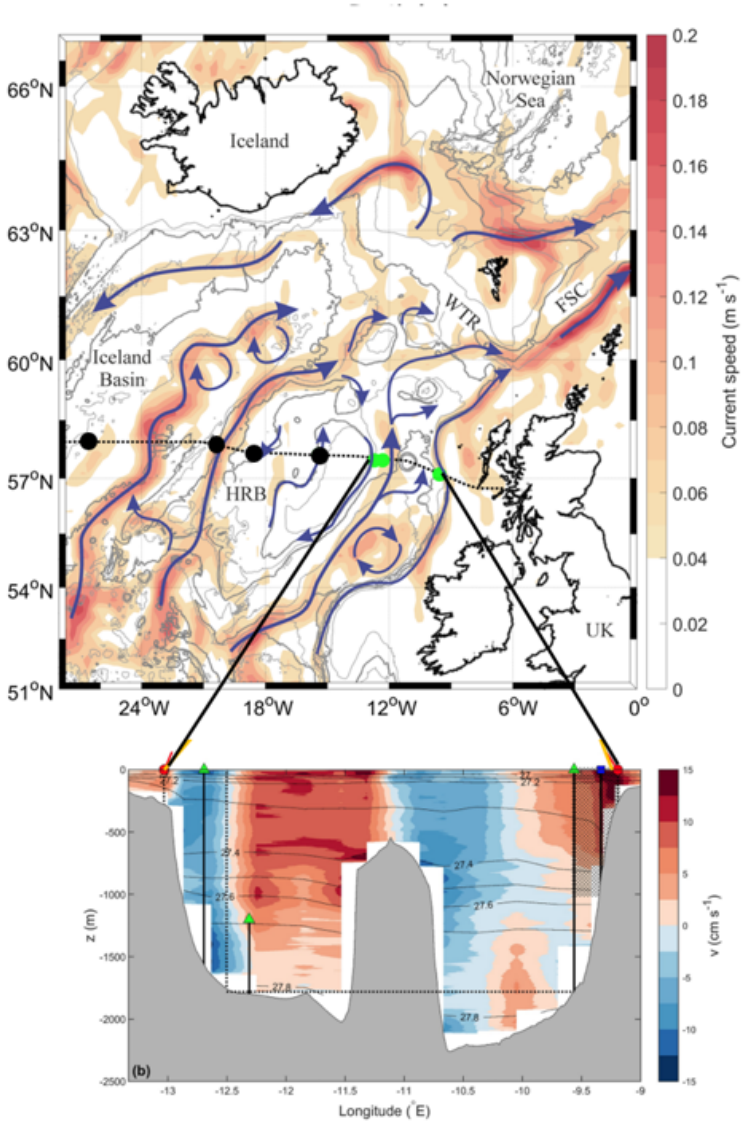

Figure 1. a) 1993-2023 mean satellite-derived surface current speed and schematic of North Atlantic upper ocean circulation (blue arrows), as well as position of the Ellett Array (black and green circles), from west to east: IB3 (discontinued since 2024), IB4, IB5, RHADCP, RTWB1, RTWB2, RTEB1. The full Ellett Array is shown for completeness, this study focusses on the RT moorings only (green circles). b) Solid vertical black lines show mooring locations and the dotted vertical line at -12.5°E marks the partition between the western wedge and mid-basin regions, defined as the midway point between WB1 and WB2. Black cross-hatching in the upper 1,000 m of the eastern wedge denotes the region monitored by gliders. Shading shows mean meridional (positive northward) velocity in the RT from 17 repeat lowered acoustic Doppler current profiler sections along the Extended Ellett Line in the period 1996–2017, while black contours show the corresponding potential density values (previously presented in Fraser et al., 2022; Houpert et al., 2020).

https://doi.org/10.5194/egusphere-2025-3167
Preprint. Discussion started: 25 July 2025

vector perpendicular to the glider path is assigned to the same isobath onto the common section and rotated to become perpendicular to the common section. This value is then scaled by the steepness of the seabed along the glider path relative to the steepness of the seabed on the common section. This second step ensures that the transport between two given isobaths is conserved. Transformed values are interpolated onto a two-dimensional grid with horizontal and vertical resolutions $dx \sim 250\,\mathrm{m}$ and $dz = 10\,\mathrm{m}$ respectively using the (Barnes, 1994) objective analysis method. We employ horizontal and vertical smoothing length scales of 3 km and 10 m, respectively. Meridional velocity is computed from gridded temperature and salinity fields via the thermal wind relation and referenced using the gridded DAC values. While this method addresses the spatial scatter of glider data, the hydrographic and velocity transects remain scattered and sparse in time. The Fraser et al. (2022) product is therefore limited for long-term continuous monitoring of the ESC.

2.2 Moored observations

Moored hydrographic and velocity observations are obtained from three hydrographic subsurface moorings (WB1, WB2, EB1) at either side of the RT from 2014 to 2022 (Houpert et al., 2020; Fraser et al., 2022). All moorings are equipped with Sea-Bird SBE37MP CTDs and Nortek Aquadopp single point current meters distributed throughout the water column (Figure 2). Figure 1 shows the location and depth of the different moorings: EB1 (57.1°N, 9.6°W) and WB1 (57.5°N, 12.7°W) are full-depth moorings extending from the seabed (EB1 at 1800 m, WB1 at 1600 m) to about 50 m. WB2 (57.5°N, 12.3°W) is located downslope of WB1 at 1800 m water depth to extend the western boundary observation to the same depth as EB1. We concatenate WB1 and WB2 hydrography to generate a virtual mooring, WB1/2, located at the midpoint between WB1 and WB2 (12.5°W) (Houpert et al., 2020).

Temperature and salinity data are corrected for sensor drift pre- and post-deployment using in-situ CTD profiles. Over a two year deployment period, the accuracy of the calibrated moored salinity, temperature and pressure data are estimated to be 0.003, 0.002°C and 1dbar, respectively (McCarthy et al., 2015). Temperature and salinity data are then linearly interpolated on to a regular 2-hour time grid and de-spiked. Horizontal velocity measurements are corrected for sound and magnetic deviation.

The corrected hydrographic data are de-tided using a 48-hr lowpass filter, then linearly interpolated on a 20-dbar vertical grid and a 12-hr temporal grid. The gridded temperature and salinity fields were extrapolated to the surface by repeating the uppermost observed values vertically at each time step. The observed velocity fields are linearly extrapolated to the surface (Houpert et al., 2020; Fraser et al., 2022).

The data return of the moored hydrographic and velocity instruments are generally very high (see black solid lines marking pressure records of each instrument in Figure 2). A summary of the different gab filling methods applied to the gridded mooring data over the years is given in the supplementary information (see section S1).

A bottom-mounted acoustic Doppler current profiler (RTADCP) was deployed in the ESC core in 2014 but the instrument was lost after around 8 months (Houpert et al., 2020).

https://doi.org/10.5194/egusphere-2025-3167
Preprint. Discussion started: 25 July 2025

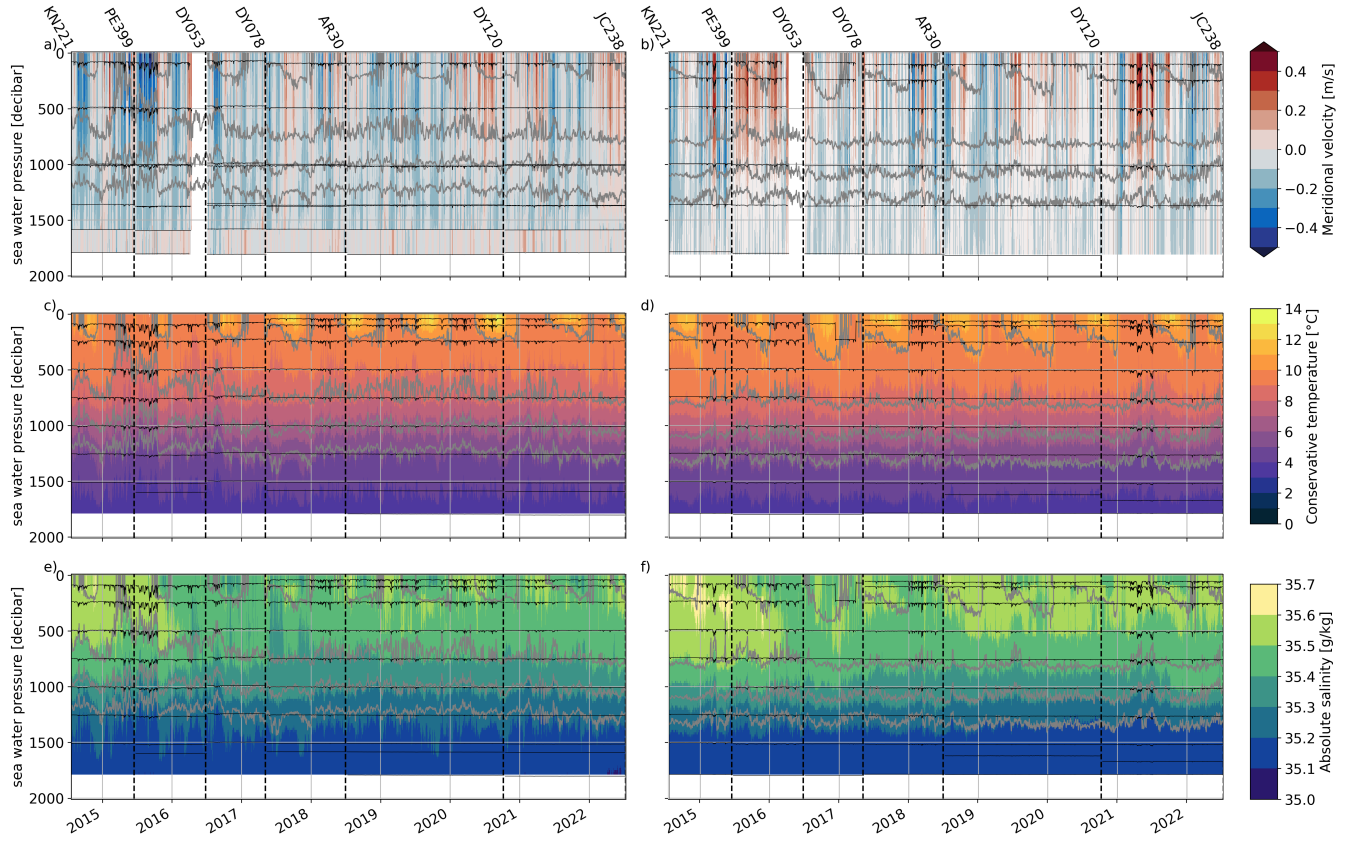

Figure 2. Gridded fields of moored meridional velocity (a-b), conservative temperature (c-d) and absolute salinity (e-f) of WB1/2 (a,c,e) and EB1 (b,d,f). Black lines mark the pressure time series for the single current meters (a-b) and CTD sensors (d-f). Grey contour lines show potential density values at 27.2, 27.4, 27.6 and 27.7 kg m^{-3} (top to bottom). Vertical dashed black lines indicate the individual servicing cruises for the moorings.

2.3 Supplementary data

For the eastern RT boundary region, meridional velocity fields from the Global Ocean Physics Reanalysis GLORYS12V1 for the period July 2014 to July 2022 were obtained from the Copernicus Marine and Environment Monitoring Service (CMEMS). GLORYS21V1 is a global ocean eddy-resolving (1/12° horizontal resolution, 50 vertical levels) reanalysis covering the altimetry period (1993 onward).

Gridded bathymetry data were obtained at 30 arc-second resolution from the General Bathymetric Chart of the Ocean (GEBCO) version 20141103.

https://doi.org/10.5194/egusphere-2025-3167
Preprint. Discussion started: 25 July 2025

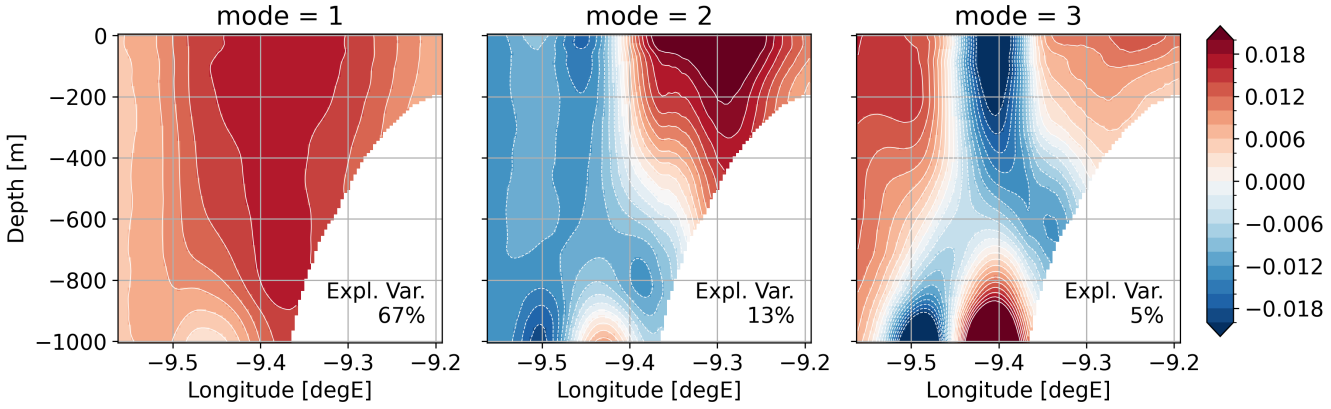

Figure 3. First 3 EOF patterns derived from 166 glider-based meridional velocity observations along the eastern wedge section between 2020 and 2023.

3 Transport calculations

Volume, heat and freshwater transports through the RT are calculated as the sum of the transports in the western wedge, the mid-basin and the eastern wedge. We present a new methodology for calculating eastern wedge transport which utilises both mooring and glider observations. For comparison, we also compute eastern wedge transport using the previous methodology (Houpert et al., 2020). We derive western wedge and mid-basin transports as in previous studies (Houpert et al., 2020; Fraser et al., 2022).

3.1 Eastern wedge velocity from glider and mooring observations

Gliders capture the RT eastern wedge velocity field with high spatial resolution, while moored EB1 current meters offer excellent temporal resolution and longer-term coverage (from 2014 onward in this instance). This motivates a combined approach that leverages the strengths of both datasets. We are guided by the methodology of Brandt et al. (2014, 2016, 2021), who integrate long-term mooring observations with high-resolution ship sections to construct a comprehensive velocity product.

We use empirical orthogonal function (EOF) analysis to identify the dominant modes of variability in the eastern wedge velocity field, based on 166 glider transects (Figure 3). The first EOF explains 67% of the total variance and represents a coherent strengthening or weakening of the entire section, with peak amplitudes between 9.3°W and 9.5°W. Near-zero values appear below 800 m between 9.4°W and 9.5°W, corresponding to the core of a southward-flowing undercurrent (Fraser et al., 2022).

The second EOF explains 13% of the variance and highlights variability centered east of 9.4°W, associated with the mean position of the ESC, with opposite-sign amplitudes to the west. The undercurrent also appears in this mode, exhibiting contrasting amplitudes on either side of its mean core location. Higher-order EOF modes (mode 3 and above) explain less than 6% of the variance individually and display more complex, less interpretable patterns. Overall, the EOF results indicate that

https://doi.org/10.5194/egusphere-2025-3167
Preprint. Discussion started: 25 July 2025

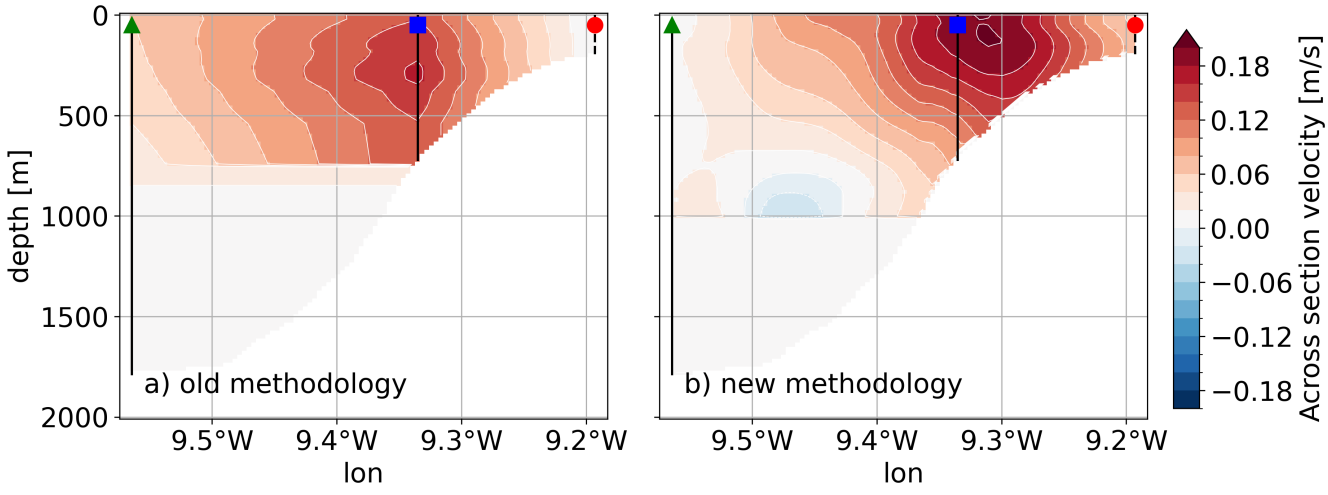

Figure 4. Averaged across section velocity for the eastern wedge using a) old methodology from Houpert et al. (2020) and Fraser et al. (2022) and b) the new methodology including glider observations. Black line with green triangle marks mooring EB1, black line with blue square marks the position of the ADCP, dashed black line with red dot marks the eastern limit of the section.

the dominant variability in the ESC is primarily due to temporal strengthening and weakening, rather than spatial shifts in its position.

A parallel analysis was performed using Hilbert EOFs, which can in theory account for spatially propagating features in the velocity field. However, the results were not substantively different from those obtained using standard EOFs.

The second step of the eastern wedge velocity field reconstruction is to regress the EOF patterns ($X(x,z)$) onto the meridional velocities from the EB1 mooring and the GLORYS2v1 output at the RTADCP location. We seek a velocity section for each time step of the meridional velocity time series, $v(x,z,t)$, such that

$$v(x,z,t) = X(x,z) \cdot \alpha(t) \tag{1}$$

We must therefore obtain the regression coefficient α. We combine the meridional velocities from EB1 and GLORYS2v12 at each time step to give $v_{loc}(t)$, select values of the EOF pattern at the location of EB1 and RTADCP to get X_{loc} and find $\alpha(t)$ using a least squares solution:

$$\alpha(t) = (X_{loc}^T X_{loc})^{-1} X_{loc}^T v_{loc}(t). \tag{2}$$

To validate the new methodology we compare the resulting transports with those calculated from the original, temporally-scattered glider sections. The glider transport time series reconstructed using only the first EOF has a correlation of $R = 0.90$ and a root-mean-square-error (RMSE) of 0.79 Sv compared to the original glider transports. Using the first two EOFs results

https://doi.org/10.5194/egusphere-2025-3167
Preprint. Discussion started: 25 July 2025

in a lower agreement ($R = 0.88$, RMSE$= 0.87$ Sv). We repeated the same validation by reconstructing the velocity field using only glider data at EB1 and the first EOF, to explore if we can reconstruct the transport without relying on GLORYS12V1 output. However, this decreased the correlation between the reconstructed transport and the original glider transports to $R = 0.48$ and increased the RMSE to 2.63 Sv.

We conclude that best results are obtained by using the first EOF pattern of the glider sections in combination with observed velocities at EB1 and GLORYS12V1 output at RTADCP for the reconstruction of the velocity field of the upper 1000 m of the eastern wedge section. The velocity field below 1000 m is constructed by repeating gridded velocities from EB1 horizontally eastward into the seabed (Figure 4b). The volume, heat and freshwater transports are then calculated from the reconstructed eastern wedge velocity and hydrography sections using Equations 3-5.

3.2 Eastern wedge velocity - previous methodology

We briefly review the method used in earlier studies (Fraser et al., 2022; Houpert et al., 2020).

Houpert et al. (2020) found that the GLORYS12V1 ocean reanalysis accurately captured the variability in an 8-month time series of meridional velocity measured by the RTADCP during its first deployment. However, the reanalysis consistently underestimated the flow strength by approximately +7.6 cm s^{-1}. To correct for this bias, they interpolated the GLORYS12V1 meridional velocities to the RTADCP location (57.1°N, 9.3°W, upper 750 m) and applied a uniform offset of +7.6 cm s^{-1}.

In the old method, the meridional velocities from GLORYS12V1 and the gridded EB1 data were linearly interpolated between EB1 and the RTADCP location for depths shallower than 750 m. East of RTADCP, the GLORYS12V1 velocities were tapered linearly to zero at 9.2°W, marking the eastern end of the section. For depths below 750 m, the gridded EB1 velocities were extended horizontally eastward to the seabed (Figure 4a).

3.3 Western wedge and mid-basin velocity

For the reconstruction of the western wedge and mid-basin transport through the RT, we follow the methodologies of Houpert et al. (2020) and Fraser et al. (2022). The velocity field for the western wedge is reconstructed using the gridded meridional velocity from WB1/2 and extents from 12.5°W to 13°W . To represent the horizontally uniform flow in the ship-board velocity observations (Figure 1), WB1 current meter values are replicated eastward to the WB1/2 position. West of WB1, velocities deeper than 250 m are tapered linearly to zero at the seabed, while velocities above 250m are tapered linearly to reach zero at 12.9°E to omit the northward jet over the Rockall Bank centred at 13°W (Figure 1 and SI Figure 2).

The mid-basin transport per unit depth at each depth level is derived from the difference in the dynamic heights, referenced to the deepest shared level of 1760 m, between EB1 and WB1/2 (Fraser et al., 2022).

3.4 Total volume, heat and freshwater transport

We calculate the volume, heat and freshwater transport as follows.

https://doi.org/10.5194/egusphere-2025-3167
Preprint. Discussion started: 25 July 2025

The volume transport Q is calculated by spatially integrating a velocity field:

$$Q = \int_{-H}^{0} \int_{x_1}^{x_2} v\,(x,z)\; dx\, dz \tag{3}$$

where v is the velocity component perpendicular to the section, x and z are the along-section and depth coordinates, x_1 and x_2 are the section endpoints and H is water depth.

The heat transport Q_h is given by

$$Q_h = \rho_{ref} C_p \int_{-H}^{0} \int_{x_1}^{x_2} v\,(x,z)\,(\Theta(z) - \Theta_{ref})\; dx\, dz \tag{4}$$

where $\rho_{ref} C_p = 4.1 \cdot 10^6\,\mathrm{J\,m^{-3}\,C^{-1}}$ is the product of the reference density and specific heat capacity, and $\Theta_{ref} = 7.07\,^{\circ}\mathrm{C}$ is the reference conservative temperature. For the western wedge, $\Theta(z)$ is the temperature profile of WB1/2, for the mid-basin $\Theta(z)$ is the average temperature profile of WB1/2 and EB1 and for the eastern wedge, $\Theta(z)$ is the temperature profile of EB1.

The freshwater transport Q_f is calculated as follows:

$$Q_f = \int_{-H}^{0} \int_{x_1}^{x_2} \left(v\,(x,z)\, \frac{S(z) - S_{ref}}{S_{ref}} \right) dx\, dz \tag{5}$$

where $S_{ref} = 35.34\,\mathrm{g\,kg^{-1}}$ is the reference absolute salinity and $S(z)$ is the absolute salinity profile from WB1/2, the average salinity profile of WB1/2 and EB1, and the salinity profile from EB1 for the western wedge, the mid-basin and the eastern wedge, respectively.

4 Results

We first focus on the ESC, investigate its mean strength and variability in glider and moored observations and assess the continuous transport reconstruction for the eastern wedge section. We then examine the 8-year records of volume, heat and freshwater transport for the full RT section.

4.1 ESC from glider and moored observations 2020-2022

The extension of the Ellett Array dataset to 2022 provides, for the first time, a temporal overlap between glider and moored observations of the ESC. This allows a direct comparison of transport estimates in the upper 1000 m from glider-derived velocities and from mooring-based reconstructions using both the previous and current methods.

All three estimates show good agreement (Figure 5), with both reconstructions correlating well with glider-derived transport (both $R = 0.8$). However, extreme transport events observed by the gliders—e.g., in December 2020 and May 2021—are suppressed in both reconstructions.

https://doi.org/10.5194/egusphere-2025-3167
Preprint. Discussion started: 25 July 2025

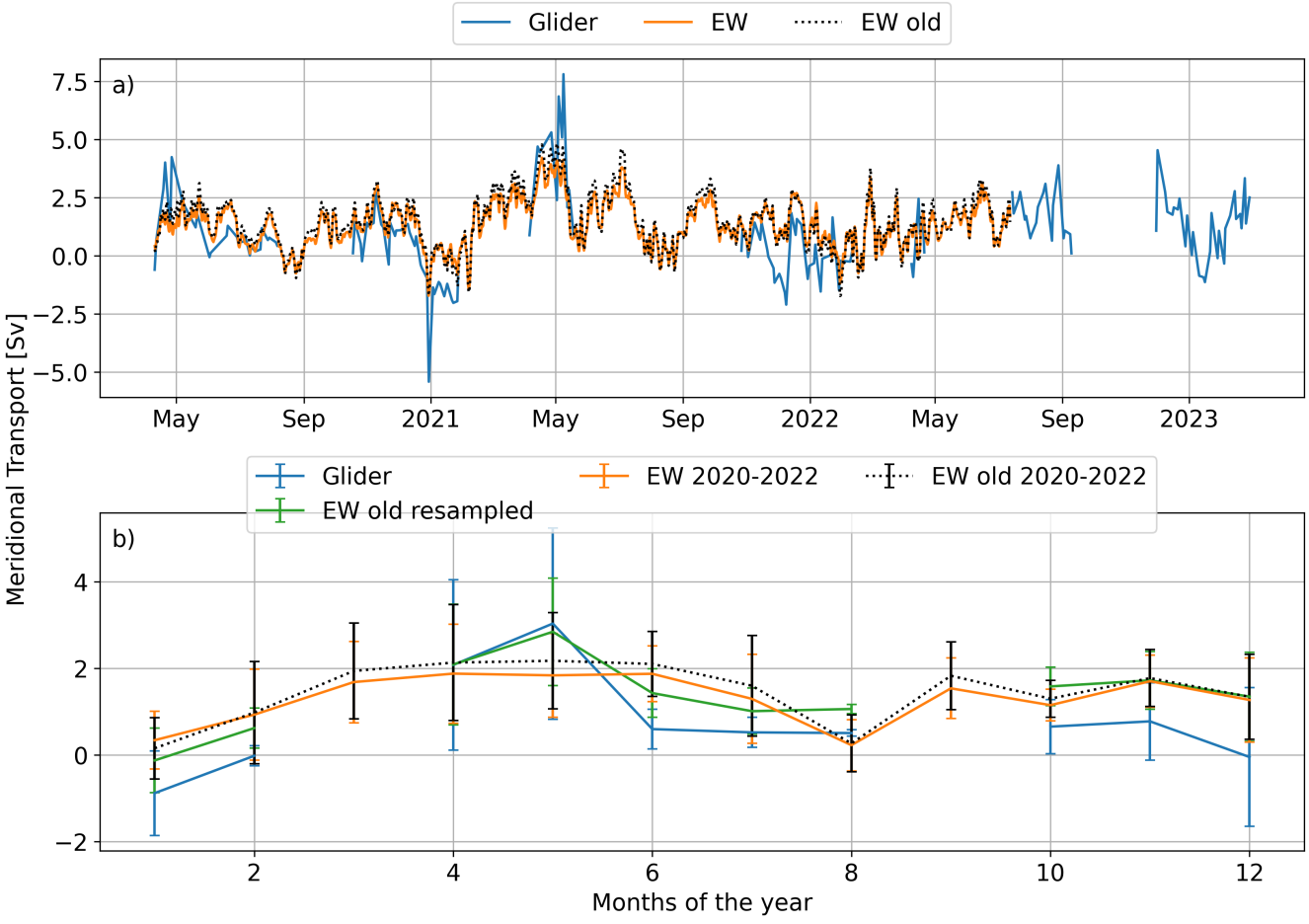

Figure 5. Time series of meridional velocities depth-averaged for the upper 1000m derived for the eastern wedge section from moored observations and GLORYS12V1 model output (orange line) and glider observations (blue line). Different time intervals were used as noted in legend. For glider (blue) and old methodology resampled (green) only periods when data are available in both time series are used to calculate seasonal cycle.

https://doi.org/10.5194/egusphere-2025-3167
Preprint. Discussion started: 25 July 2025

During the period of overlap, mean transports differ notably, with transport values of 1.4 ± 0.3 and 1.3 ± 0.3 for the previous and current methods respectively, compared to 0.8 ± 0.4 Sv for the individual glider sections. This discrepancy may be due to the previous method's inability to resolve the southward undercurrent below 750 m. The current method partially captures this feature, though it still overestimates the mean transport relative to the gliders by 0.5 Sv—just outside the glider's standard error.

Both reconstructions depend on a bias correction to GLORYS12v1, derived from a limited 8-month calibration period (2014–2015). When the bias correction is omitted, the mean transport drops to 0.7 ± 0.3 Sv, aligning more closely with glider estimates. The low glider-derived mean between April 2020 and April 2022 is influenced by a single extreme event in December 2020 (< -5 Sv), which neither reconstruction captures. Extending the averaging period to February 2023 increases the glider mean to 1.0 ± 0.3 Sv, in better agreement with the bias-corrected reconstruction.

Sparse and irregular glider sampling—especially gaps in March and September—limits seasonal resolution. Seasonal cycles (Figure 5b) show a May peak in the glider data, absent from reconstructions over the full overlap period. However, this peak appears when the previous reconstruction method is resampled to glider time steps, driven by the strong positive transports in May 2021. Over the full mooring period (2014–2022), the seasonal cycle shows a January minimum, a secondary August minimum, and enhanced transports in spring, early summer, and late autumn.

4.2 RT volume, heat and freshwater transports 2014-2022

The northward volume transport through the RT has a mean (± 1 standard error) of 4.7$\pm$0.5 Sv between 2014 and 2022 (Figure 6a), which is within the uncertainty of previous transport calculations for shorter periods (Houpert et al., 2020; Fraser et al., 2022). As in these previous studies, the mid-basin dominates the volume transport with a mean of 5.0$\pm$0.5 Sv, while the western and eastern wedges have mean northward volume transports of -1.5$\pm$0.3 Sv and 1.3$\pm$0.2 Sv respectively. For both heat and freshwater transports, the mid-basin accounts for about 70% while the eastern wedge accounts for about 30% and the western wedge contribution is small (Figure 6b-c).

We find a decreasing trend of -0.40 Sv/yr in the mid-basin volume transport which is mostly balanced by a increasing trend (i.e. reduced southward flow) of 0.29 Sv/yr in the western wedge. The eastern wedge volume transport is fairly constant. This results in a trend of -0.13 Sv/yr for the total volume transport, which is small given the large range of values in the time series (> 10 Sv). We find trends of -0.10 $\times 10^{-2}$PW/yr in northward heat transport and 0.14 $\times 10^{-2}$Sv/yr of northward freshwater transport (i.e. less freshwater transported south).

The RT volume transport displays variability on the order of several Sverdrups on intraseasonal to interannual time scales, as reported in previous studies (Houpert et al., 2020; Fraser et al., 2022). Volume transport largely explains the patterns of variability in heat ($R = 0.90$) and freshwater transports ($R = -0.84$). For the 9-month low-pass filtered time series we find a significant anti-correlation of $R = -0.3$ between the mid-basin and western wedge volume transports. The eastern wedge volume transport is not correlated with either the mid-basin or western wedge, which indicates that the ESC is dynamically distinct from the NAC branch in the RT. The mid-basin dominates the variability in total volume transport, with a correlation of $R = 0.74$ based on the 9-month low pass filtered time series.

https://doi.org/10.5194/egusphere-2025-3167
Preprint. Discussion started: 25 July 2025

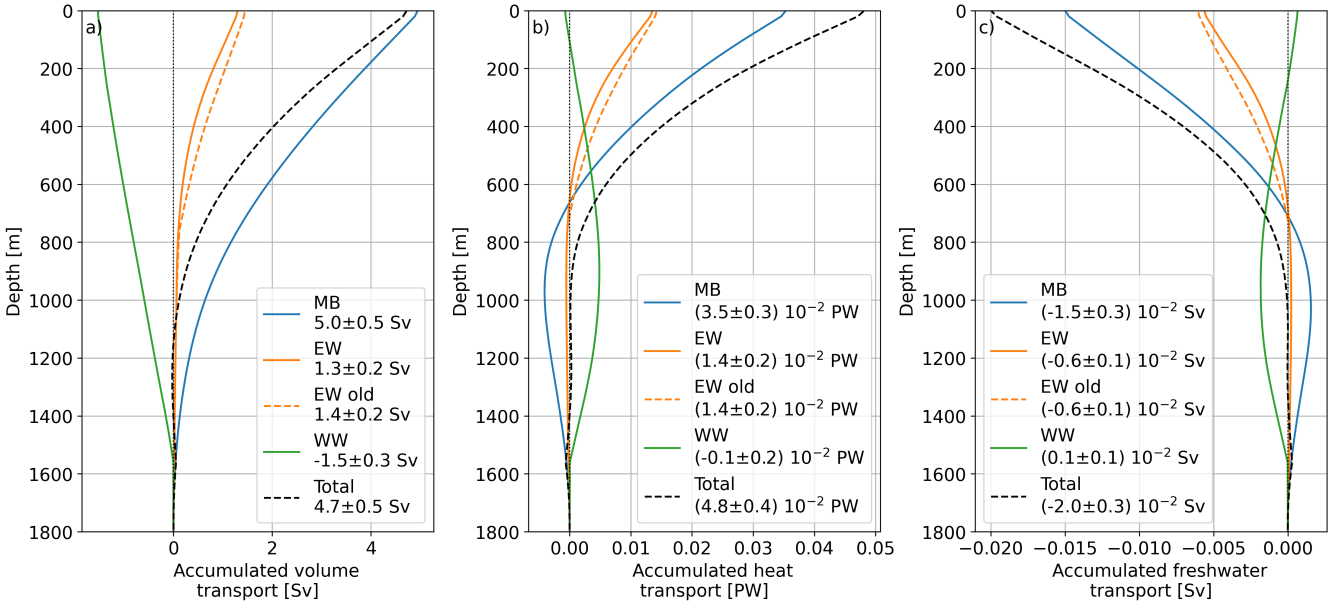

Figure 6. Depth-accumulated mean a) volume, b) heat and c) freshwater transports in the RT. Values are shown for the mid basin (MB) in blue, the eastern wedge (EW) in orange (solid for the new, dashed for the old methodology), the western wedge (WW) in green and the total transport in black.

On multiannual time scales, the variability of the heat and freshwater transport appears qualitatively similar to the volume transport (Figure 7b,d,f). However, by highlighting extreme interannual events (defined as when the 9-month low-pass filtered time series exceeds the temporal averaged transport by $\pm$ 1 standard deviation) we show that volume and heat transports largely co-vary, but freshwater transport exhibits a different pattern. Before 2016 the southward freshwater transports are relatively high, while after 2017 the southward freshwater transports are reduced with only one period of extreme high.

Fraser et al. (2022) suggest that the low salinity values in 2017 mark the arrival of the mid-2010s subpolar freshwater anomaly (Holliday et al., 2020; Fox et al., 2022) in the northern RT. The updated time series shows that, by 2022, the salinity values have only partially recovered to their pre-2017 maximum (Figure 2). However, these low salinities do not strongly impact the total volume transport (Figure 8a). By isolating the contribution from temperature and salinity in the eastern and western boundaries, Fraser et al. (2022) found that the transport minimum during 2017 was instead due to high subsurface temperature anomalies which occurred only in the western basin (Figure 8 and SI Figure 2). Performing the same analysis with the extended record reveals that the low transport events in 2019 and 2021 are due to low subsurface temperature anomalies at the eastern RT boundary (Figure 8 and SI Figure 2).

https://doi.org/10.5194/egusphere-2025-3167
Preprint. Discussion started: 25 July 2025

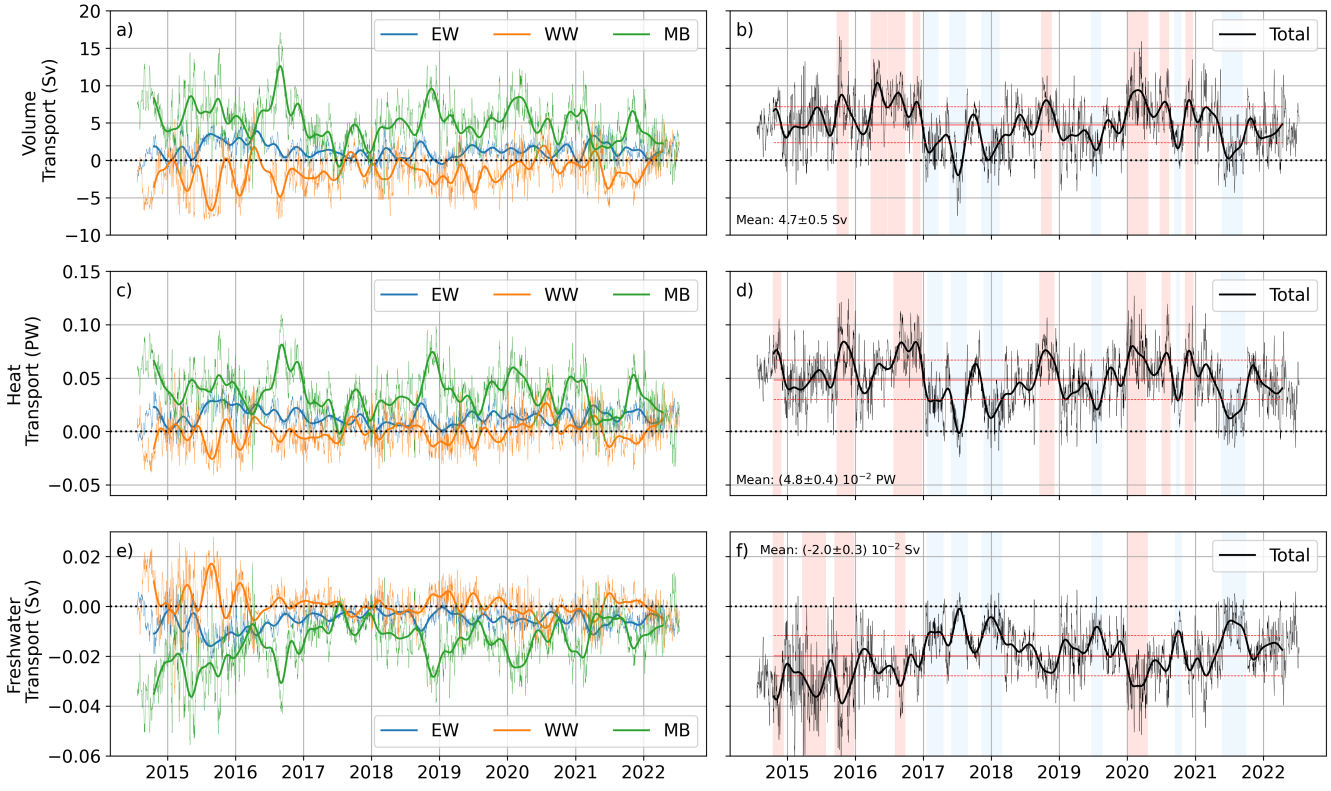

Figure 7. RT volume, heat and freshwater transports for eastern wedge (blue), western wedge (orange), mid-basin (green) and total (black). Red solid lines mark the mean total volume, heat and freshwater transport and the dashed read lines mark ±1STD.

5 Discussion

We present the RT circulation and fluxes observed by the Ellett Array from 2014 to 2022. As well as extending the volume transport time series reported previously (Houpert et al., 2020; Fraser et al., 2022), we also present the associated heat and freshwater fluxes for the first time. Until now, the glider observations at the eastern boundary were not integrated into the full RT transport product due to their inconsistent temporal coverage. In this study, we developed a methodology to calculate eastern boundary transports by utilising the high spatial resolution from gliders together with the high temporal resolution provided by moorings and numerical model output. The resulting velocity fields are then easily integrated in the full RT transport product.

Our new methodology leads to a better representation of the eastern boundary current system in the RT velocity fields and provides a robust seasonal cycle (Figure 5). In particular, the method captures the southward undercurrent which was not resolved by the horizontal interpolation approach used previously (Figure 4), resulting in reduced northward transport at the eastern boundary (Figure 6a). Our method still requires ancillary data from a numerical model, albeit calibrated against direct velocity observations. A longer temporal overlap between the glider and mooring observations would facilitate better calibration, and we suggest this should be the focus of future research.

https://doi.org/10.5194/egusphere-2025-3167
Preprint. Discussion started: 25 July 2025

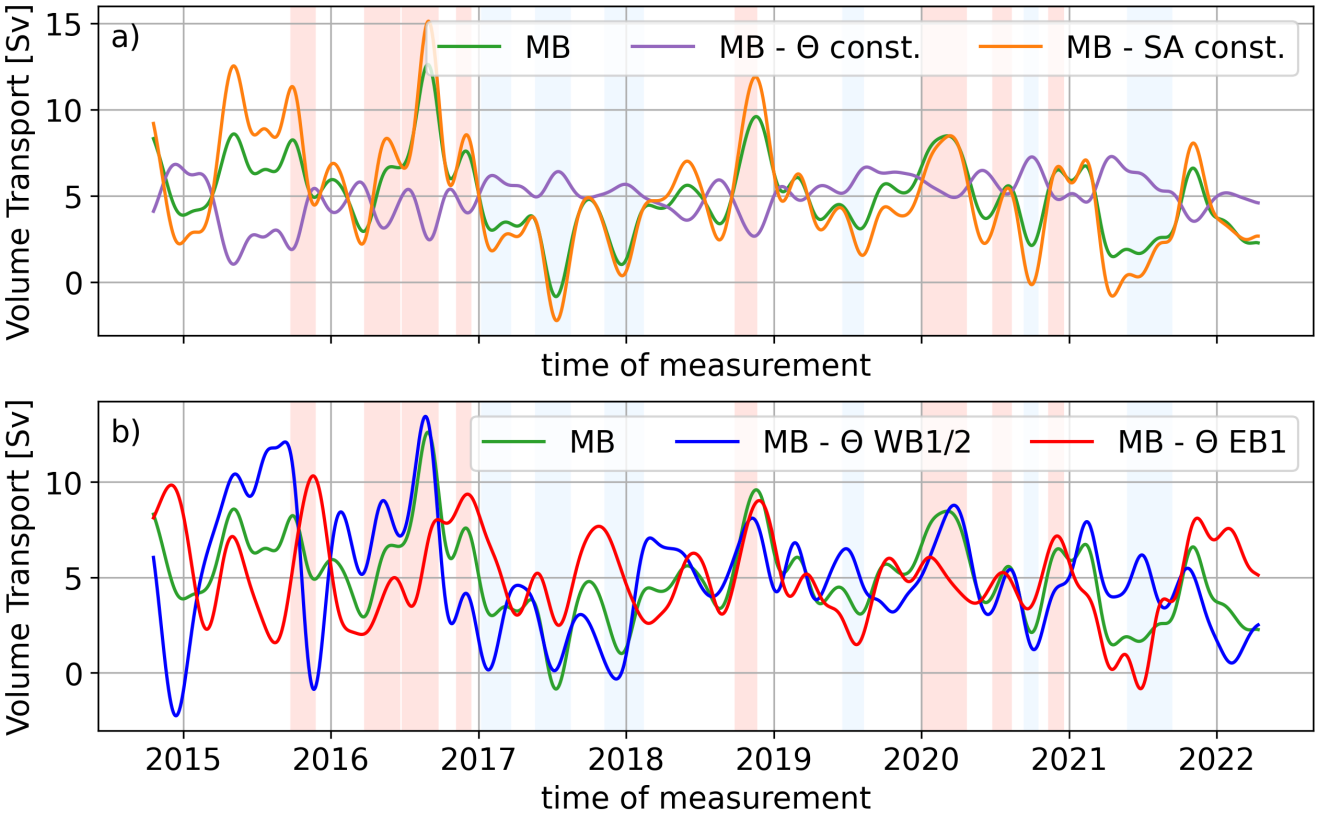

Figure 8. Time series of 9-month low-pass filtered volume transport through mid-basin (a) isolating changes in salinity (purple line) or temperature (orange line) and (b) isolation changes in temperature at WB1/2 (blue line) or EB1 (red line). The green line shows the mid-basin volume transport as shown in Figure 7 for reference. Red (blue) patches mark the total RT volume transport exceeding (deciding) the temporal mean+1STD (−1STD) (red solid and dashed lines).

The RT volume transport displayed substantial interannual variability during 2014-2022 but no significant trend. This is because declining northward transport in the mid-basin was counteracted by decreasing southward flow at the western boundary. Interannual variability of the NAC strength in the RT mid-basin is controlled the interplay of subsurface temperature anomalies at the eastern and western boundaries (Figure 8 and SI Figure 2). While the variability in northward heat flux is closely tied to volume transport (Figure 7), the (southward) freshwater transport weakens over the record, indicating the influence of salinity changes operating on longer timescales.

Variability in the ESC appears to be independent from that of the NAC in the mid-basin (Figure 8a). Although the ESC has a relatively small mean transport, it is disproportionately important for poleward heat and freshwater fluxes through the RT (Figure 6).

https://doi.org/10.5194/egusphere-2025-3167
Preprint. Discussion started: 25 July 2025

This study highlights the value of targetted observing systems for delivering accurate, continuous records of ocean circulation required for Atlantic climate monitoring. Gliders provide unique insights into boundary currents which would be difficult to achieve with traditional platforms. When integrated with mooring data using the methodology presented here, they become a powerful, complementary component of the Ellett Array observing system. Our approach can be directly applied to the more general problem of ocean transport monitoring using a heterogeneous array of mooring and glider platforms.

Code and data availability. Code available on github: https://github.com/ScotMarPhys/Rockall_Trough_Transports/tree/master. Rockall Trough data: https://thredds.sams.ac.uk/thredds/catalog/osnap/catalog.html. GLORYS12v2 link:https://data.marine.copernicus.eu/product/GLOBAL_MULTIYEAR_PHY_001_030/description, doi: https://doi.org/10.48670/moi-00021. GEBCO version 20141103 link: https://www.gebco.net/data_and_products/gridded_bathymetry_data/version_20141103/. Altimetry data link: https://data.marine.copernicus.eu/product/SEALEVEL_GLO_PHY_CLIMATE_L4_MY_008_057/description, doi: https://doi.org/10.48670/moi-00145.

Author contributions. KB planned and performed the analysis. KB, NJF and SCJ authored the paper. KB, LAD and SCJ post-processed the mooring and glider data. SAC, MEI and NPH secured funding for the research. All co-authors contributed to the scientific improvement of the paper.

Competing interests. The contact author has declared that none of the authors has any competing interests.

Disclaimer. This output reflects only the author's view, and the European Union cannot be held responsible for any use that may be made of the information contained therein.

Acknowledgements. We thank the captains, crews, scientists, and technical groups involved in the different national and international research cruises, on research vessels RRS Discovery and RRS James Cook to the subpolar North Atlantic for their contributions in collecting CTD, velocity, and mooring data and for making them freely available. This project was supported by the UK Natural Environment Research Council National Capability programme AtlantiS (NE/Y005589/1), NERC Grants UK OSNAP (NE/K010875/1 and NE/ K010875/2), UK OSNAP Decade (NE/T00858X/1) and ODISSEA (NE/Y005236/1). This project has received funding from the European Union's Horizon 2020 research and innovation programme under grant agreement No. 818123 (iAtlantic).

https://doi.org/10.5194/egusphere-2025-3167
Preprint. Discussion started: 25 July 2025

References

Barnes, S. L.: Applications of the Barnes Objective Analysis Scheme. Part II: Improving Derivative Estimates, Journal of Atmospheric and Oceanic Technology, 11, 1449–1458, https://doi.org/10.1175/1520-0426(1994)011<1449:AOTBOA>2.0.CO;2, 1994.

Berx, B., Hansen, B., Østerhus, S., Larsen, K. M., Sherwin, T., and Jochumsen, K.: Combining in situ measurements and altimetry to estimate volume, heat and salt transport variability through the Faroe–Shetland Channel, Ocean Science, 9, 639–654, https://doi.org/10.5194/os-9-639-2013, 2013.

Brandt, P., Funk, A., Tantet, A., Johns, W. E., and Fischer, J.: The Equatorial Undercurrent in the central Atlantic and its relation to tropical Atlantic variability, Climate Dynamics, 43, 2985–2997, https://doi.org/10.1007/s00382-014-2061-4, 2014.

Brandt, P., Claus, M., Greatbatch, R. J., Kopte, R., Toole, J. M., Johns, W. E., and Böning, C. W.: Annual and Semiannual Cycle of Equatorial Atlantic Circulation Associated with Basin-Mode Resonance, Journal of Physical Oceanography, 46, 3011–3029, https://doi.org/10.1175/JPO-D-15-0248.1, 2016.

Brandt, P., Hahn, J., Schmidtko, S., Tuchen, F. P., Kopte, R., Kiko, R., Bourlès, B., Czeschel, R., and Dengler, M.: Atlantic Equatorial Undercurrent intensification counteracts warming-induced deoxygenation, Nature Geoscience, 14, 278–282, https://doi.org/10.1038/s41561-021-00716-1, 2021.

Daly, E., Nolan, G., Berry, A., Büscher, J. V., Cave, R. R., Caesar, L., Cronin, M., Fennell, S., Lyons, K., McAleer, A., McCarthy, G. D., McGovern, E., McGovern, J. V., McGrath, T., O'Donnell, G., Pereiro, D., Thomas, R., Vaughan, L., White, M., and Cusack, C.: Diurnal to interannual variability in the Northeast Atlantic from hydrographic transects and fixed time-series across the Rockall Trough, Deep Sea Research Part I: Oceanographic Research Papers, 204, 104 233, https://doi.org/10.1016/j.dsr.2024.104233, 2024.

Diabaté, S. T., Fraser, N. J., White, M., Berx, B., Marié, L., and McCarthy, G. D.: On the wind-driven European shelf sea-level variability and the associated oceanic circulation, Continental Shelf Research, 291, 105 466, https://doi.org/https://doi.org/10.1016/j.csr.2025.105466, 2025.

Ellett, D. J., Edwards, A., and Bowers, R.: The hydrography of the Rockall Channel—an overview, Proceedings of the Royal Society of Edinburgh. Section B. Biological Sciences, 88, 61–81, https://doi.org/10.1017/S0269727000004474, 1986.

Eriksen, C., Osse, T., Light, R., Wen, T., Lehman, T., Sabin, P., Ballard, J., and Chiodi, A.: Seaglider: a long-range autonomous underwater vehicle for oceanographic research, IEEE Journal of Oceanic Engineering, 26, 424–436, https://doi.org/10.1109/48.972073, 2001.

Fox, A. D., Biastoch, A., Cunningham, S. A., Fraser, N., Handmann, P., Holliday, P., Johnson, C., Martin, T., Oltmanns, M., Rath, W., Rühs, S., Sanchez-franks, A., and Schmidt, C.: Exceptional freshening and cooling in the eastern subpolar North Atlantic caused by reduced Labrador Sea surface heat loss, pp. 1–35, 2022.

Fraser, N. J., Cunningham, S. A., Drysdale, L. A., Inall, M. E., Johnson, C., Jones, S. C., Burmeister, K., Fox, A. D., Dumont, E., Porter, M., and Holliday, N. P.: North Atlantic Current and European Slope Current Circulation in the Rockall Trough Observed Using Moorings and Gliders, Journal of Geophysical Research: Oceans, 127, https://doi.org/10.1029/2022JC019291, 2022.

GLORYS12V1: Global Ocean Physics Reanalysis. E.U. Copernicus Marine Service Information (CMEMS). Marine Data Store (MDS). (Accessed on 16-May-2024), https://doi.org/10.48670/moi-00021.

Gregor, L., Ryan-Keogh, T. J., Nicholson, S.-A., du Plessis, M., Giddy, I., and Swart, S.: GliderTools: A Python Toolbox for Processing Underwater Glider Data, Frontiers in Marine Science, 6, https://doi.org/10.3389/fmars.2019.00738, 2019.

Holliday, N. P., Bersch, M., Berx, B., Chafik, L., Cunningham, S., Florindo-López, C., Hátún, H., Johns, W., Josey, S. A., Larsen, K. M. H., Mulet, S., Oltmanns, M., Reverdin, G., Rossby, T., Thierry, V., Valdimarsson, H., and Yashayaev, I.: Ocean circulation causes the largest

https://doi.org/10.5194/egusphere-2025-3167
Preprint. Discussion started: 25 July 2025

freshening event for 120 years in eastern subpolar North Atlantic, Nature Communications, 11, 585, https://doi.org/10.1038/s41467-020-14474-y, 2020.

Holliday, P. and Cunningham, S.: The Extended Ellett Line: Discoveries From 65 Years of Marine Observations West of the UK, Oceanography, 26, https://doi.org/10.5670/oceanog.2013.17, 2013.

Houpert, L., Cunningham, S., Fraser, N., Johnson, C., Holliday, N. P., Jones, S., Moat, B., and Rayner, D.: Observed Variability of the North Atlantic Current in the Rockall Trough From 4 Years of Mooring Measurements, Journal of Geophysical Research: Oceans, 125, 1–9, https://doi.org/10.1029/2020JC016403, 2020.

Jones, S., Inall, M., Porter, M., Graham, J. A., and Cottier, F.: Storm-driven across-shelf oceanic flows into coastal waters, Ocean Science, 16, 389–403, https://doi.org/10.5194/os-16-389-2020, 2020.

Jones, S. C., Fraser, N. J., Cunningham, S. A., Fox, A. D., and Inall, M. E.: Observation-based estimates of volume, heat, and freshwater exchanges between the subpolar North Atlantic interior, its boundary currents, and the atmosphere, Ocean Science, 19, 169–192, https://doi.org/10.5194/os-19-169-2023, 2023.

Lozier, M. S., Li, F., Bacon, S., Bahr, F., Bower, A. S., Cunningham, S. A., de Jong, M. F., de Steur, L., DeYoung, B., Fischer, J., Gary, S. F., Greenan, B. J. W., Holliday, N. P., Houk, A., Houpert, L., Inall, M. E., Johns, W. E., Johnson, H. L., Johnson, C., Karstensen, J., Koman, G., Bras, I. A. L., Lin, X., Mackay, N., Marshall, D. P., Mercier, H., Oltmanns, M., Pickart, R. S., Ramsey, A. L., Rayner, D., Straneo, F., Thierry, V., Torres, D. J., Williams, R. G., Wilson, C., Yang, J., Yashayaev, I., and Zhao, J.: A sea change in our view of overturning in the subpolar North Atlantic, Science, 363, 516–521, https://doi.org/10.1126/science.aau6592, 2019.

Marsh, R., Haigh, I. D., Cunningham, S. A., Inall, M. E., Porter, M., and Moat, B. I.: Large-scale forcing of the European Slope Current and associated inflows to the North Sea, Ocean Science, 13, 315–335, https://doi.org/10.5194/os-13-315-2017, 2017.

McCarthy, G., Smeed, D., Johns, W., Frajka-Williams, E., Moat, B., Rayner, D., Baringer, M., Meinen, C., Collins, J., and Bryden, H.: Measuring the Atlantic Meridional Overturning Circulation at 26°N, Progress in Oceanography, 130, 91–111, https://doi.org/10.1016/j.pocean.2014.10.006, 2015.

Porter, M., Dale, A., Jones, S., Siemering, B., and Inall, M.: Cross-slope flow in the Atlantic Inflow Current driven by the on-shelf deflection of a slope current, Deep Sea Research Part I: Oceanographic Research Papers, 140, 173–185, https://doi.org/10.1016/j.dsr.2018.09.002, 2018.